

Molecular Dynamics Simulation on Interacting and Mechanical Properties of Polylactic Acid and Attapulgite(100) Surface

Su-Qin Zhou, Xiao-Chun Cheng, Ye-Ling Jin, Jie Wu, Deng-Shan Zhao

Key Laboratory for Attapulgite Science and Applied Technology of Jiangsu Province, Faculty of Life Science and Chemical Engineering, Huaiyin Institute of Technology, Huaian 223003, People's Republic of China
 Correspondence to: X.-C. Cheng (E-mail: chengxc126@126.com)

ABSTRACT: The method of molecular dynamics (MD) simulations was used to investigate the interaction between the PLA and the attapulgite, and the influence of the temperature on the mechanical properties of the PLA and the PLA-attapulgite. After the PLA blends the attapulgite, the structures and properties of the PLA and the attapulgite change due to their strong interaction. However, this interaction weakens gradually with temperature increasing. The isotropy of the composite of PLA-attapulgite is strengthened in comparison with the PLA. In addition, the temperature can change the mechanical properties of the PLA-attapulgite, but the mechanical properties of the PLA are hardly influenced on the temperature. The PLA-attapulgite is more rigid and tough than the PLA at the room temperature but the toughness of the composite of PLA-attapulgite becomes worse than that of the PLA at 350 K.
 © 2012 Wiley Periodicals, Inc. *J. Appl. Polym. Sci.* 000: 000–000, 2012

KEYWORDS: theory and modeling; surfaces and interfaces; mechanical properties

Received 19 April 2012; accepted 19 August 2012; published online

DOI: 10.1002/app.38492

INTRODUCTION

Polylactic acid (PLA) is a chain aliphatic, thermoplastic and biodegradable polyester produced from renewable resources. However, some properties of PLA like low melt viscosity, low heat distortion temperature, and bad gas barrier limit its various applications.^{1–5} The PLA nanocomposites based on layer silicates of montmorillonite, sepiolite, calcium sulfate and calcium carbonate were prepared to overcome these limitations.^{5–10} At present, attapulgite, as polymer additive, has attracted wide attention all over the world. Attapulgite can reinforce benefits of epoxy polymer, for example, improvements in tensile properties at low loadings levels of 2 and 5% (w/w) and increasing the viscosity of the prepolymer.¹¹ Compared with neat polyamide 6 (PA6), tensile strength of attapulgite (ATB)/PA6 composites reaches a maximum value with incorporation of 4 wt % ATB and bending strength reaches a maximum value with incorporation of 2 wt % attapulgite. There are strong interactions between ATB and PA6.¹² The addition of attapulgite can improve the heat distortion temperature and Young's modulus of poly(butylene succinate) nanocomposites.¹³ The attapulgite enhance mechanical properties of polyurethane, reinforce its shape-memory and decrease glass transition temperature and hardness due to the presence of moisture as well as the clay's structure and surface hydroxyl groups.¹⁴ Although there were

reports of the attapulgite/polymer composites, there are no experimental and theoretical studies on the attapulgite/PLA.

Computer simulations have played an important role in the field of materials. Simulations may provide an understanding of the structure–performance relationships in materials, which in turn can help design better and more efficient experiment. A force field method, especially molecular dynamics (MD) method, is an important and effective method to study the structure and performance of materials at present.^{15,16}

In this article, we investigate the interaction of attapulgite and PLA, and predict their mechanical properties at the different temperature by molecular dynamics (MD) method. It is hoped that our studies provide some information and guidance for attapulgite/PLA composites formulation design.

MATERIALS AND METHODS

Experimental Materials and Instrumentation

The PLA and the attapulgite (100) surface were selected as the investigated system. The cubic box of the PLA is processed by the amorphous cell module of the Accelrys materials studio (MS) software.¹⁷ Its box contains 902 atoms and the box size is 2.101 nm × 2.101 nm × 2.101 nm. Thus the density of the obtained PLA is 1.29 g cm⁻³, which is consistent with the one of the PLA crystal.¹⁸ The PLA is made up of a chain of $\text{-(O-CH-CH}_2\text{)-}_n$



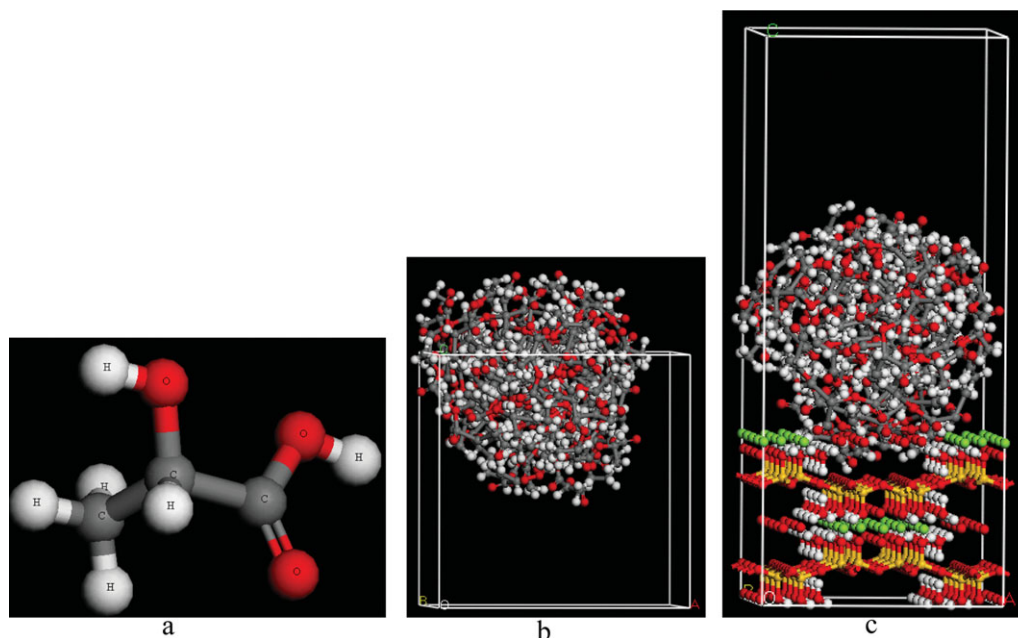


Figure 1. (a) Structure of lactic acid; (b) Initial configuration of poly-lactic-acid 902 atoms; (c) Initial configuration of interacting with poly-lactic-acid and attapulgite (100) surface 503 atoms. [Color figure can be viewed in the online issue, which is available at wileyonlinelibrary.com.]

($n = 100$), whose end groups are saturated by two H atoms. The attapulgite (100) surface of a $1 \times 4 \times 1$ super-cell containing 503 atoms is constructed from orthorhombic attapulgite crystal,¹⁹ which contains 32 H₂O molecules, 51 Mg atoms, 64 Si atoms, H atoms of Si—O—H bond and O atoms. Finally, the attapulgite (100) surface of 503 atoms and the PLA of 902 atoms are assembled together by the “build layers” command of MS software. The box for the compound of the attapulgite and the PLA is separated from the attapulgite (100) surface by 3.0 nm of vacuum along c axes, and the box size with cubic box of $a \times b \times c$ is $1.79 \text{ nm} \times 2.08 \text{ nm} \times 4.21 \text{ nm}$. The density for the compound of the PLA-attapulgite is 1.48 g cm^{-3} .

The models of the PLA and the attapulgite (100) surface were constructed on Pentium IV computer by the amorphous cell module of the Accelrys materials studio (MS) software,¹⁷ based on the experimental data of the PLA and the attapulgite crystal. In addition, all MD simulation computations of the constructed models were performed on 36-CPU cluster computers by the Discovery module of the Accelrys materials studio (MS) software.

Simulation Methods

Smart minimizer method was initially carried out for 10,000 iterations to equilibrate the system. Starting from the final minimized structure, the MD simulations were subsequently carried out with the temperature of 300, 350, and 400 K at the pressure of 0.1 GPa. All MD simulations were performed in the NVT ensemble (constant number of particles, volume, and temperature) with the COMPASS force field.²⁰ The periodic box of the PLA and the box with the composite of PLA and attapulgite were simulated 1.4 ns with the MD method. The first 1.0 ns is to get the equilibrium configurations, and during the latter 0.4 ns 200 trajectories data are collected for subsequent analysis. A fixed time step size of 1 fs (1×10^{-15} s) was used in all cases. The Andersen thermostat method²¹ was employed to control the sys-

tem at all temperatures. In all of the simulations, periodic nature of the crystal has been considered by using periodic boundary conditions in all dimensions, and the equations of motion for the molecules and simulation cells were integrated using the Verlet leapfrog scheme.²² The interactions were determined between the sites in the simulation box and the nearest-image sites within the cutoff distance 0.95 nm. The Coulomb and van der Waals long-range, nonbond interactions were handled by using the standard Ewald and atom-based summation methods, respectively.²³ The electrostatic charges were determined and assigned automatically by the selected COMPASS force field. We have tested the influence of atomic charges on the crystal structures and properties by manually scaling the charges of atoms in the unit cell based on the COMPASS force-field-assigned charges. It was found that there is a little discrepancy between the predicted results from the force-field-assigned charges and manually assigned specific charges. All simulations are performed by Discover module.²⁴ In all simulations, atoms under lower Mg atoms of the attapulgite were fixed, other atoms of the upper layers for attapulgite and PLA were relaxed. Figure 1 gives the structure of the lactic acid, the initial configuration of the PLA and the initial configuration of interacting between the PLA and the attapulgite (100) surface.

RESULTS AND DISCUSSION

Equilibrium Configuration

After the MD simulations, we give the equilibrium configurations with the temperature of 300, 350, and 400 K at the pressure of 0.1 GPa. Figure 2 gives the equilibrium configurations of the PLA with the temperature of 300, 350, and 400 K at the pressure of 0.1 GPa. Figure 3 gives the equilibrium configurations for the composite of PLA-attapulgite with the temperature of 300, 350, and 400 K at the pressure of 0.1 GPa.

From Figure 2, the configurations of PLA become incompact, compared to the initial one [i.e., Figure 1(b)]. The

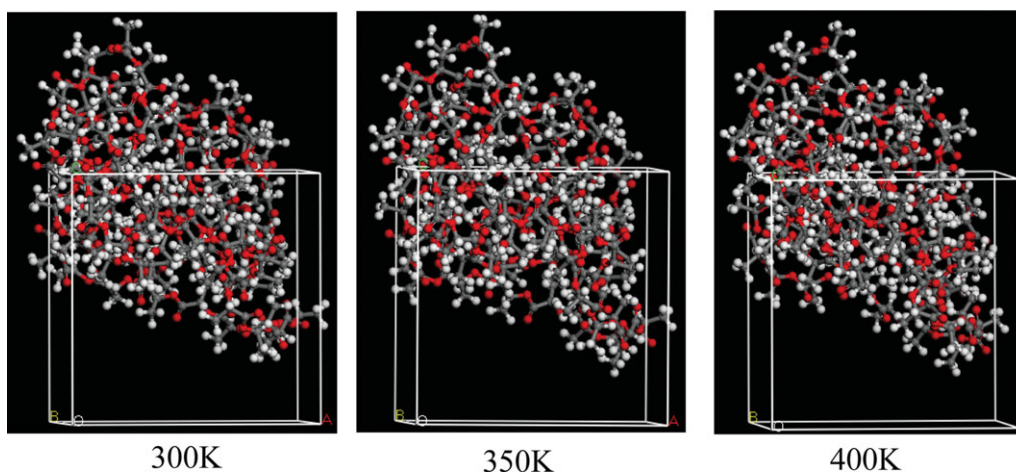


Figure 2. The equilibrium configurations of different temperature after MD at the pressure of 0.1 GPa for the poly-lactic-acid. [Color figure can be viewed in the online issue, which is available at wileyonlinelibrary.com.]

configurations of different temperature are similar to each other. This shows the influence of the temperature on the structure of the PLA is small. From Figure 3, the PLA become incompact; the relaxed Mg, O (except O atoms of Si—O bond) atoms and some relaxed H₂O molecules of the attapulgite diffuse away from the attapulgite (100) surface to the PLA. What's more, the Si—O and Si—O—H bonds of the relaxed distort badly. With increasing temperature, these changes are not obvious. This infers the temperature affect little the structure of the PLA and the attapulgite.

Binding Energy

The binding energy can accurately reflect the features for different composites. The molecular interaction can be evaluated by the single point total energy of each component in the stable system, and the average binding energy (E_{bind}) between the PLA

and the attapulgite can be expressed as eq. (1),

$$E_{\text{bind}} = E_{\text{total}} - (E_{\text{PLA}} + E_{\text{attapulgite}}) \quad (1)$$

Where E_{total} is the average total energy for the composite of PLA and attapulgite, E_{PLA} and $E_{\text{attapulgite}}$ are the average single point energy for the PLA and the attapulgite, respectively.

Table I gives the binding energy of the PLA and the attapulgite. As seen from Table I, the largest binding energy (E_{bind}) is -991.2 kcal at 300 K, but the smallest one is -883.3 kcal at 400 K. The E_{bind} decreases with increasing temperature at the pressure of 0.1 GPa, which indicates the interacting between the PLA and the attapulgite becomes weak with temperature increasing.

Radial Distribution Functions

The interaction of PLA and attapulgite can be further analyzed by the radial distribution functions (RDF). The RDF has many

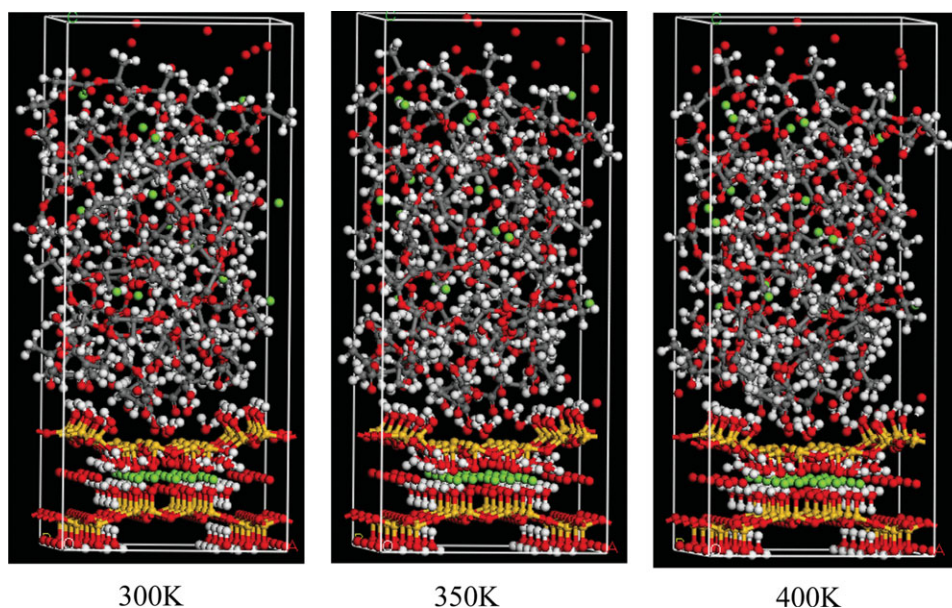


Figure 3. The equilibrium configurations of different temperature after MD at the pressure of 0.1 GPa for interacting with poly-lactic-acid and attapulgite (100) surface. [Color figure can be viewed in the online issue, which is available at wileyonlinelibrary.com.]

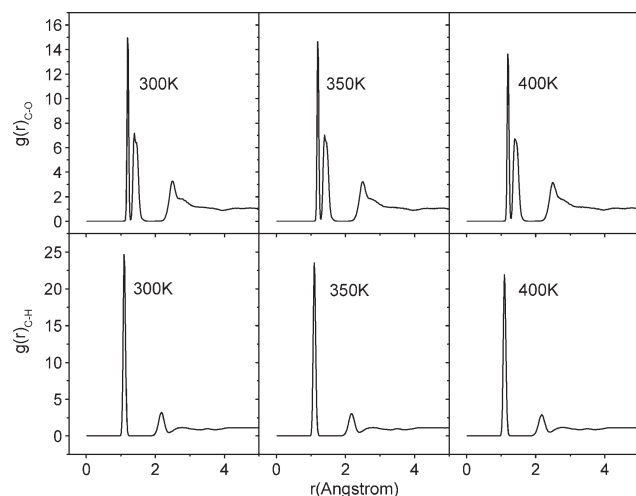
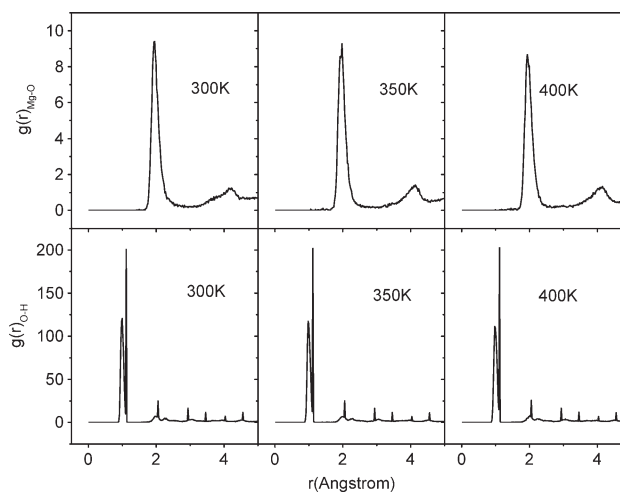
Table I. Binding Energy (E_{bind}) between the Polylactic Acid and the Attapulgite

Temperature (K)	300	350	400
$E_{\text{bind}}/\text{kcal}$	-991.2	-920.0	-883.3

applications in structural investigations of both solid and liquid packing (local structure), in studying specific interactions, and in statistical mechanical theories of liquids and mixtures.^{25,26} A more quantitative analysis can be performed using RDF that correlates the relative positions of selected atoms or atomic centers of mass. The RDF values for C atoms with O and H atoms of the PLA were shown in Figure 4. Whereas, Figure 5 gives the RDF values for Mg atoms with O atoms of the PLA and O atoms with H atoms of Si—O—H bonds.

As seen from Figure 4, the first peak of $g(r)$ for C—O of the PLA appears at the 1.13–1.25 Å, and the C=O bond length (1.22 Å) is within this distance range. The second one appears at the 1.25–1.75 Å, and the C—O bond length (1.43 Å) lies within the distance range. The third one is at the 1.95–3.00 Å, and this length range corresponds to the length of the non-bonding C—O. The first peak of $g(r)$ for C—H of the PLA appears at the 0.95–1.22 Å, and the C—H bond length (1.09 Å) is within this distance range. The second one appears at the 1.90–2.35 Å, and this length range corresponds to the length of the nonbonding C—H. As the temperature increases, all peak values for $g(r)$ decreases gradually. This shows the intra-action of the PLA weakens gradually with temperature increasing.

From Figure 5, the peak values of $g(r)$ for Mg atoms with O atoms of the PLA are 1.75–2.25 Å and 4.00–4.25 Å, respectively. The highest peak value of $g(r)$ for O—H of the Si—O—H bonds is 0.89–1.13 Å. At large values of r , $g(r)$ goes to 1. Based on these data and Figure 5, it can be concluded that Mg atoms of the attapulgite diffuse to the PLA and the interacting of Mg atoms with O atoms of the PLA is very strong, which indicates the interacting between the PLA and the attapulgite is also strong. In addition, the interacting between the PLA and the

**Figure 4.** The radial distribution function for C atoms with O and H atoms of polylactic acid at different temperature.**Figure 5.** The radial distribution function for Mg atoms of the attapulgite with O atoms of the polylactic acid, and O atoms with H atoms of the Si—O—H bonds at different temperature.

attapulgite becomes weak with temperature increasing because the highest peak values of $g(r)$ for Mg atoms O atoms decrease with the temperature increasing. However, the O—H bond length of the Si—O—H bonds changes slightly.

Mechanical Properties

Based on the NVT-MD simulation trajectories, each structure is subjected to uniaxial tensile and pure shear deformations by the elastic-static method, and then the stress tensors are obtained from the Virial formalism in atomistic calculations. Consequently, the elastic coefficient matrix can be estimated from the first derivatives of the stress with respect to strain.²⁷ The tensile (Young's) modulus and Poisson ratio are computed from the least-square fits of the average tensile stress versus tensile strain and of the average lateral strain versus tensile strain, respectively. Other effective isotropic mechanical properties such as the bulk modulus, shear modulus, and Lamé coefficients then can be obtained correspondingly.

Generalized Hook's law states the most general relation of a material between stress and strain; that is, a stress can be expressed by the linear combination of strains, and the coefficient C_{ij} is an element of the elastic coefficient matrix of 6×6 . In principle, all mechanical properties of a material can be derived from its elastic coefficient matrix. Because of the existence of strain energy, the elastic coefficient matrix of a bulk should satisfy the formula $C_{ij} = C_{ji}$ even for an extremely anisotropic body, and there are 21 independent elastic constants. The symmetry can further reduce the number of independent elastic coefficients. For an isotropic solid, there are only two independent elastic constants. Accordingly, each modulus and Poisson's ratio can be obtained from two Lamé coefficients (λ and μ). The static method in MS program assumes each material to be isotropic and accordingly gives effective isotropic mechanical properties.

The predicted elastic constants and effective isotropic mechanical properties (tensile modulus, bulk modulus, shear modulus, and Poisson ratio) were collected in Table II for the PLA and the composite of PLA-attapulgite, respectively. Because up to now

Table II. Elastic Constants C_{ij} and Mechanical Properties of PLA and PLA-Attapulgit (in GPa)

Element	PLA			PLA-attapulgit		
	300	350	400	300	350	400
Temperature (K)	300	350	400	300	350	400
C_{11}	116.56	122.68	68.66	189.27	155.45	202.95
C_{22}	109.28	114.45	63.05	186.54	155.99	210.67
C_{33}	118.04	126.17	74.06	2.26	83.41	-4.14
C_{44}	44.37	45.80	23.17	30.32	61.05	38.90
C_{55}	46.32	45.84	27.59	14.43	41.27	18.48
C_{66}	44.43	45.85	21.97	32.29	8.86	46.72
C_{12}	24.78	26.68	11.87	119.94	120.41	109.39
C_{13}	26.12	27.07	17.64	44.97	-34.74	53.64
C_{23}	26.00	26.48	15.94	48.65	-45.34	53.76
C_{15}	-0.54	-0.74	-2.96	-58.01	43.52	90.22
C_{25}	1.47	0.48	-0.45	-42.33	38.96	91.07
C_{35}	-1.27	-0.78	-0.92	64.24	-65.63	-70.01
C_{46}	0.70	1.12	0.14	-1.74	-6.66	-0.65
Tensile modulus (E)	105.40	111.54	63.55	104.56	129.32	99.65
Bulk modulus (K)	55.16	58.06	31.65	45.88	67.84	54.20
Shear modulus (G)	44.60	47.28	27.71	64.84	41.16	64.22
Poisson's ratio (ν) ^a	0.18	0.18	0.16	0.14	0.02	0.09
K/G ^a	1.24	1.23	1.140	1.41	0.69	1.18
$C_{12}-C_{44}$	-19.59	-19.12	-11.30	89.61	59.36	70.49

^aTheir units are 1.

there are no experimental and theoretical studies on their stress-strain relationships, we cannot make any comparison but only compare the results of the composite of PLA-attapulgit with those of the neat PLA. In comparison with other smaller elastic constants, the larger diagonal elements of the tensor C_{ii} and C_{12} , C_{13} , C_{23} indicate that the crystal PLA has considerable anisotropy. For the composite of PLA-attapulgit, C_{11} , C_{22} and C_{12} are larger than other elastic constants. The larger C_{11} , C_{22} , and C_{12} imply that, to reach the same strain, the composite of PLA-attapulgit need a larger stress. A majority of elastic constants (except C_{55} , C_{15} , C_{46} , and C_{25}) of the PLA increase first, and then decrease with temperature increasing. What's more, some elastic constants (C_{33} , C_{44} , C_{55} , and C_{12}) of the composite of PLA-attapulgit increase first, and then decrease with temperature increasing. The C_{11} , C_{22} , and C_{12} of the composite of PLA-attapulgit are larger than those of the crystal PLA at the same temperature, whereas some elastic constants (C_{33} , C_{55} , and C_{66}) are smaller than those of PLA. This average tendency of elastic coefficients shows that the anisotropy of the composite of PLA-attapulgit is weakened as blending the bulk attapulgit in small quantities, namely, the isotropy of the composite of PLA-attapulgit is strengthened in comparison with the PLA. This is mainly that because the attapulgit is mineral and has random cores, which have good isotropic properties. What's more, the elastic constants of the PLA decrease obviously when the temperature reaches 400 K. This is because the PLA starts to melt when the temperature is close to the melting point (448 K).

As can be also seen from Table II, tensile modulus (E) and bulk modulus (K) for the composite of PLA-attapulgit are larger

than those of the pure PLA at the temperature of 350 and 400 K. On the contrary, E and K of PLA-attapulgit are smaller than those of the pure PLA at 300 K. The shear modulus (G) for the composite of PLA-attapulgit is larger than those of the PLA at the temperature of 300 and 400 K, whereas G for the composite of PLA-attapulgit is smaller than that of the PLA at 350 K. These indicate that the composite of PLA-attapulgit is more rigid than the PLA at room temperature, while the elasticity and plasticity of the composite of PLA-attapulgit are worse than those of the PLA at room temperature. Meanwhile, these variations also suggest that the composite of PLA-attapulgit deform hardly and is broken easily at room temperature, because the resistance to plastic deformation is proportional to the elastic shear modulus G and the fracture strength for materials is proportional to the bulk modulus K .²⁸ Poisson's ratio (ν) of the PLA is 0.18 at the temperature of 300 and 350 K, and the ν are 0.16 at 400 K. With temperature increasing, the ν of the PLA decrease slightly. This shows the influence of temperature on rigid and plastic properties of the PLA is small. As compared to the PLA, the ν of PLA-attapulgit decrease from 300 to 400 K. Commonly, the Poisson's ratio of a plastic is 0.2–0.4. Thus, it is further demonstrated that the composite of PLA-attapulgit possesses more rigid than the PLA. Meanwhile, this indicates the influence of temperature on rigid or plastic properties for the composite of PLA-attapulgit is obvious.

Additionally, the ratio of bulk modulus to shear modulus, that is, K/G , is an indication of the extent of the plastic range for a material. A higher value of K/G is associated with toughness and a lower value with brittleness.²⁸ According to this, it can be

deduced from the K/G values in Table II that the toughness of the PLA change hardly with temperature increasing, while the toughness for the composite of PLA-attapulgitite become better at 300 K in comparison with PLA. In addition, the toughness of the composite of PLA-attapulgitite becomes worse at 350 K. This indicates the temperature influences the toughness of the composite of PLA-attapulgitite.

On the other hand, the Cauchy pressure ($C_{12}-C_{44}$) can be used as a criterion to evaluate the toughness or brittleness of a material. As a rule, the ($C_{12}-C_{44}$) value of a toughness material is positive, contrarily, the negative value corresponding to a brittle material. Meanwhile, the more positive the ($C_{12}-C_{44}$) value is, the more tough the material is. According to this, the data in the last column of Table II indicate that the PLA is brittle due to its negative ($C_{12}-C_{44}$) at the temperature of 300 to 400 K, whereas the composite of PLA-attapulgitite is toughness due to its positive ($C_{12}-C_{44}$), which agrees well with the conclusion drawn from the G and K/G .

The glass transition temperature of the PLA is at the range of 328–423 K, and the melting point of the PLA is 448 K. The temperature can change the state of the PLA. It can be concluded that the temperature can influence the mechanical properties of PLA and PLA-attapulgitite. The temperature of 300 K is very close to the room temperature, i.e., the service temperature of PLA, and the temperature of 400 K is among the range of the glass transition temperature. Therefore, the maximum or minimum of the mechanical properties of PLA and PLA-attapulgitite is in the temperature range of 300–400K.

Synthetically considering all moduli, the poisson's ratio, the ratio of bulk modulus to shear modulus and the Cauchy pressure, mechanical properties of the PLA change slightly when the temperature is from 300 to 350 K. However, mechanical properties of the PLA change obviously when the temperature reaches 400 K. The mechanical properties for the composite of PLA-attapulgitite are different from each other at the temperature of 300–400 K. Compared to the PLA, the toughness of PLA-attapulgitite is strengthened at room temperature.

CONCLUSION

The interaction and mechanical properties of the PLA and the attapulgitite have been investigated by the molecular dynamics method. The major findings can be summarized as follows.

1. When the PLA blends the attapulgitite, the PLA become incompact; the Mg, O (except O atoms of Si—O bond) atoms and some H₂O molecules of the attapulgitite diffuse away from the attapulgitite (100) surface to the PLA. As the temperature increases, the diffusion of these atoms and molecules increases, too. The Si—O and Si—O—H bonds distort badly.
2. The maximum binding energy (E_{bind}) is -991.2 kcal at 300 K, and the minimum one is -883.3 kcal at 400 K. The E_{bind} decreases with the temperature increasing at the pressure of 0.1 GPa, which indicates the interacting between the PLA and the attapulgitite weakens with the temperature increasing.
3. As the temperature increases, all peak values of $g(r)$ decreases for the PLA. This shows the intra-action of the PLA weakens with

the temperature increasing. For the PLA-attapulgitite, the highest peak value of $g(r)$ for Mg atoms with O atoms of PLA is 1.75–2.25 Å, which indicates that the interacting between the PLA and the attapulgitite is very strong. The interacting weakens gradually with the temperature increasing because the highest peak value of $g(r)$ for Mg atoms with O atoms decreases. However, the O—H bond length of the Si—O—H bonds change slightly.

4. The isotropy of the composite of PLA-attapulgitite is strengthened in comparison with the PLA. The composite of PLA-attapulgitite is more rigid and tough than the PLA at room temperature, but the toughness of the composite of PLA-attapulgitite becomes worse at 350 K. It is concluded that the temperature can change mechanical properties of the PLA-attapulgitite. However, the mechanical properties of the PLA change hardly with the temperature increasing.

ACKNOWLEDGMENTS

The authors thank support by the Natural Science Foundation of Jiangsu Province (Grant No. BK2008195), Industrial Support Plan of Jiangsu Province (Grant No. BE2009098), the Key Laboratory for Attapulgitite Science and Applied Technology of Jiangsu Province. S.-Q. Zhou thanks the Research Support of Huaiyin Institute of Technology (Grant No. HGA1008).

REFERENCES

1. Pandey, J.-K.; Raghunatha, R.-K.; Pratheep, K.-A.; Singh, R.-P. *Polym. Degrad. Stabil.* **2005**, *88*, 234.
2. Ray, S.-S.; Bousmina, M. *Prog. Mater. Sci.* **2005**, *50*, 962.
3. Ray, S.-S.; Maiti, P.; Okamoto, M.; Yamada, K.; Ueda, K. *Macromolecules* **2002**, *35*, 3104.
4. Krikorian, V.; Pochan, D. *Chem. Mater.* **2003**, *15*, 4317.
5. Emilie, P.; Eliane, E.; René, F. *Appl. Clay Sci.* **2011**, *53*, 58.
6. Ray, S.-S.; Yamada, K.; Okamoto, M.; Ogami, A.; Ueda, K. *Chem. Mater.* **2003**, *15*, 1456.
7. Paul, M.-A.; Alexandre, M.; Degée, P.; Henrist, C.; Rulmont, A.; Dubois, P. *Polymer* **2003**, *44*, 443.
8. Fukushima, K.; Tabuani, D.; Camino, G. *Mater. Sci. Eng. C* **2009**, *29*, 1433.
9. Murariu, M.; Bonnaud, L.; Yoann, P.; Fontaine, G.; Bourbigot, S.; Dubois, P. *Polym. Degrad. Stabil.* **2010**, *95*, 374.
10. Jiang, L.; Zhang, J.-W.; Wolcott, M.-P. *Polymer* **2007**, *48*, 7632.
11. Xue, S.-Q.; Reinholdt, M.; Pinnavaia, T.-J. *Polymer* **2006**, *47*, 3344.
12. Pan, B.-L.; Yue, Q.-F.; Ren, J.-F.; Wang, H.-G.; Jian, L.-Q.; Zhang, J.-Y.; Yang, S.-R. *Polym. Test.* **2006**, *25*, 384.
13. Chen, C.-H. *J. Phys. Chem. Solids* **2008**, *69*, 1411.
14. Xu, B.; Huang, W.-M.; Pei, Y.-T.; Chen, Z.-G.; Kraft, A.; Reuben, R.; De Hosson, J.-T.-M.; Fu, Y.-Q. *Eur. Polym. J.* **2009**, *45*, 1904.
15. Kumar, R.; Shinde, R.-N.; Ajay, D.; Sobhia, M.-E. *J. Chem. Inf. Model* **2010**, *50*, 1147.
16. Tosaka, R.; Yamamoto, H.; Ohdomari, I.; Watanabe, T. *Langmuir* **2010**, *26*, 9950.

17. Materials Studio 4.4. Accelrys Inc.: San Diego, CA, **2007**.
18. Garlotta, D. *J. Polym. Environ.* **2001**, *9*, 63.
19. Chisholm, J.-E. *Can. Miner.* **1992**, *30*, 61.
20. Sun, H. *J. Phys. Chem. B* **1998**, *102*, 7338.
21. Andersen, H.-C. *J. Chem. Phys.* **1980**, *72*, 2384.
22. Allen, M.-P.; Tildesley, D.-J. *Computer Simulation of Liquids*; Clarendon Press: Oxford (Hardback edition), **1987**.
23. Hansen, J.-P.; McDonald, I.-R. *Theory of Simple Liquids*; 2nd ed.; Academic Press: London, **1990**.
24. Górecki, A.; Szypowski, M.; Długosz, M.; Trylska, J. *J. Comp. Chem.* **2009**, *30*, 2364.
25. Roe, R.-J. *Encyclopedia of Polymer Science and Engineering*; Wiley: New York, **1988**.
26. Villa, A.; Peter, C.; Vegt, N.-F.-A. *J. Chem. Theory Comput.* **2010**, *6*, 2434.
27. Weiner, J.-H. *Statistical Mechanics of Elasticity*; Wiley: New York, **1983**.
28. Pugh, S.-F. *Philos. Mag.* **1954**, *45*, 823.